



Robinson, J. F., Turci, F., Roth, R., & Royall, C. P. (2019). Many-body correlations from integral geometry. *Physical Review E*, 100(6), [062126]. <https://doi.org/10.1103/PhysRevE.100.062126>

Publisher's PDF, also known as Version of record

Link to published version (if available):
[10.1103/PhysRevE.100.062126](https://doi.org/10.1103/PhysRevE.100.062126)


[Link to publication record in Explore Bristol Research](#)
PDF-document

This is the final published version of the article (version of record). It first appeared online via American Physical Society at <https://journals.aps.org/pre/abstract/10.1103/PhysRevE.100.062126> . Please refer to any applicable terms of use of the publisher.

University of Bristol - Explore Bristol Research

General rights

This document is made available in accordance with publisher policies. Please cite only the published version using the reference above. Full terms of use are available: <http://www.bristol.ac.uk/pure/user-guides/explore-bristol-research/ebr-terms/>

Many-body correlations from integral geometryJoshua F. Robinson ^{1,*} Francesco Turci,¹ Roland Roth,² and C. Patrick Royall^{1,3,4}¹*H. H. Wills Physics Laboratory, University of Bristol, Bristol BS8 1TL, United Kingdom*²*Institut für Theoretische Physik, Universität Tübingen, 72076 Tübingen, Germany*³*School of Chemistry, Cantock's Close, University of Bristol, Bristol BS8 1TS, United Kingdom*⁴*Centre for Nanoscience and Quantum Information, University of Bristol, Bristol BS8 1FD, United Kingdom*

(Received 28 August 2019; revised manuscript received 8 October 2019; published 20 December 2019)

In a recent letter we presented a framework for predicting the concentrations of many-particle local structures inside the bulk liquid as a route to assessing changes in the liquid approaching dynamical arrest. Central to this framework was the morphometric approach, a synthesis of integral geometry and liquid-state theory, which has traditionally been derived from fundamental measure theory. We present the morphometric approach in a new context as a generalization of scaled-particle theory, and we derive several morphometric theories for hard spheres of fundamental and practical interest. Our central result is a new theory that is particularly suited to the treatment of many-body correlation functions in the hard-sphere liquid, which we demonstrate by numerical tests against simulation.

DOI: [10.1103/PhysRevE.100.062126](https://doi.org/10.1103/PhysRevE.100.062126)**I. INTRODUCTION**

Since the beginning of modern liquid-state theory [1], the hard-sphere liquid has remained the archetypal model for atomic systems and soft matter. The dynamics of the system at high density in the metastable regime above the freezing transition are hotly debated, despite relentless study. Proposed mechanisms for dynamical phenomena all loosely fall under the broad umbrella of many-body correlations; nucleation occurs via crystal seed formation [2], and to explain dynamic arrest approaching the glass transition thermodynamic theories invoke cooperatively rearranging regions [3] or elastic soft modes [4], while kinetic theories posit the existence of dynamical defects [5]. In a recent letter [6] we proposed a framework for treating many-body correlations, and developed an operational scheme for predicting the populations and dynamics of local structural motifs within a uniform liquid. Central to this is the use of the *morphometric approach*.

The morphometric approach provides an efficient means of treating the thermodynamics of a bulk liquid without fully determining its equilibrium density profile [6–9]. Detailed investigations have shown that it is highly accurate in the hard-sphere liquid regime [10–15], so we can expect an accurate treatment where the bulk system provides background depletion interactions while its detailed microstates remain unimportant. This feature makes it ideally suited for many-body correlations if we can identify relevant dynamical degrees of freedom. While existing morphometric theories have been proven accurate in the liquid regime, we require a theory which works in the supercooled regime. Here we derive such a theory using scaled-particle theory (SPT).

SPT determines bulk properties from consideration of a spherical solute of varying radius. It remains one of most enduring theories of simple liquids; though 60 years old as

of this year [16], aspects of this approach remain in modern theories. This is particularly true for hard spheres where SPT has been unified with the Percus-Yevick integral equation solution [17], another old theory, in the form of fundamental measure theory (FMT) [18]. Though originally a theory of single-component hard spheres [16], SPT has been extended to other potentials [19–21] and shapes [22,23], mixtures [24], dimers [25,26], and disks [27–29]. Morphological thermodynamics can be seen as a modern generalization of SPT for a wide class of physically relevant geometries. Its basis in integral geometry replaces the semi-empirical approach of classical SPT with clearly defined postulates. In this work we present the morphometric approach in the context of SPT and derive a new theory suitable for high densities above freezing. In the Appendices, we show that minor modifications of our arguments can be used to derive previous theories: the classical SPT coefficients, and the White Bear II morphometric coefficients of Ref. [30].

In Sec. II we show how one can map the problem of treating many-body correlations onto a solvent-solute problem. We spend the rest of the paper discussing the solvation problem through the lens of SPT. We introduce the morphometric approach as a useful generalization of SPT in Sec. III, and derive a theory well-suited for treating many-body correlations using scaled-particle arguments. In Sec. IV we numerically test these theories' two- and three-body correlation functions to demonstrate their effectiveness in treating correlation functions.

II. SOLVATION EXPRESSION FOR MANY-BODY CORRELATIONS**A. Correlations in terms of the insertion cost**

We will show that correlations of n particles at positions $\vec{r}^n := \{\vec{r}_1, \dots, \vec{r}_n\}$ can be expressed in terms of the free-energy cost of inserting them at \vec{r}^n , by generalizing the

*joshua.robinson@bristol.ac.uk

potential distribution theorem [31,32] to many particles. The classical approach, also known as *Widom's insertion method*, expresses the (excess) chemical potential μ^{ex} of a single-component system as the free-energy cost of inserting an additional particle. See Ref. [33] and references therein for a detailed review of this classical approach. Our generalization results in a *potential of mean force* for interactions between the n particles, which is formally identical to the chemical potential of a solute; this latter form is particularly suitable for geometric approximation schemes.

We consider a bulk liquid (the solvent) of N particles with interaction potential energy U_N . Integrating over all solvent arrangements in the absence of any external field gives the (grand-canonical) average,

$$\langle \dots \rangle = \frac{1}{\Xi} \sum_{N=0}^{\infty} \frac{z^N}{N!} \int (\dots) e^{-\beta U_N} d\vec{r}^N,$$

with partition function $\Xi := e^{-\beta \Omega_{\text{hom}}}$, where $\Omega_{\text{hom}} = -pV$ is the usual homogeneous grand potential. The activity is $z = \exp \beta \mu / \Lambda^d$ in terms of the (total) chemical potential μ and the thermal de Broglie wavelength Λ .

Descriptions of many-body correlations naturally employ the n -particle density $\rho^{(n)}$, defined as

$$\text{Prob}[\text{any } n \text{ particles in volume } d\vec{r}^n] := \rho^{(n)}(\vec{r}^n) d\vec{r}^n. \quad (1)$$

The n -density can be obtained by integrating the full (configurational) probability distribution over the remaining degrees of freedom. For the single-component system this yields [34]

$$\rho^{(n)}(\vec{r}^n) = \frac{1}{\Xi} \sum_{N=n}^{\infty} \frac{z^N}{(N-n)!} \int e^{-\beta U_N} d\vec{r}^{(N-n)}.$$

Changing the summation limits $N \rightarrow N+n$ we obtain

$$\begin{aligned} \rho^{(n)}(\vec{r}^n) &= \frac{z^n}{\Xi} \sum_{N=0}^{\infty} \frac{z^N}{N!} \int e^{-\beta U_{N+n}} d\vec{r}^N \\ &= z^n e^{-\beta U_n} \langle e^{-\beta U_{n \leftrightarrow N}} \rangle, \end{aligned} \quad (2)$$

where in the latter step we decomposed the total potential U_{N+n} into purely local and solvent terms, i.e., $U_{N+n} = U_n + U_N + U_{n \leftrightarrow N}$, where U_α for $\alpha \in \{n, N\}$ indicates the internal interactions between particles in component α . The ‘‘inter-species’’ interactions are contained within $U_{n \leftrightarrow N}$ which acts as an external field for the solvent. Thus, Eq. (2) becomes

$$\rho^{(n)}(\vec{r}^n) = z^n e^{-\beta(U_n + \Omega - \Omega_{\text{hom}})},$$

where Ω is the grand potential of the solvent in the presence of the n -particle inhomogeneity. Splitting the chemical potential into its ideal and excess parts so that $\beta \mu = \ln \Lambda^d \rho + \beta \mu^{\text{ex}}$ gives

$$\rho^{(n)}(\vec{r}^n) = \rho^n e^{-\beta(U_n + \Omega - \Omega_{\text{hom}} - n\mu^{\text{ex}})}.$$

The n -particle distribution functions are then determined from [34]

$$g^{(n)}(\vec{r}^n) := \frac{\rho^{(n)}(\vec{r}^n)}{\rho^n} = e^{-\beta(U_n + \Delta\Omega - n\mu^{\text{ex}})}, \quad (3)$$

where $\Delta\Omega := \Omega - \Omega_{\text{hom}}$ is the reversible (free-energy) cost of inserting the particles at fixed position \vec{r}^n , or equivalently

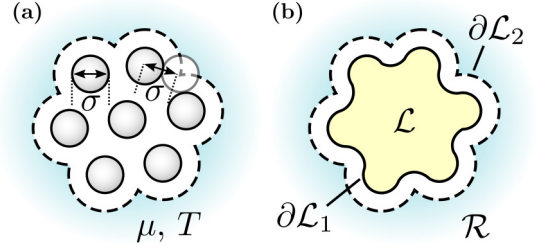


FIG. 1. The system considered for many-body correlations showing (a) the local particles surrounded by the remaining liquid acting as a thermal reservoir at fixed chemical potential and temperature and (b) possible partitions of space into the local \mathcal{L} and remaining \mathcal{R} components for two choices of dividing surface: $\partial\mathcal{L}_1$ is the molecular surface, while $\partial\mathcal{L}_2$ is the solvent accessible surface [see discussion around Eq. (10)].

describes the average depletion interactions between mobile particles. For $n = 1$ we have $\Delta\Omega = \mu^{\text{ex}}$ and this is identical to the potential distribution theorem of Widom [31,32]. The distribution functions are written in terms of the potential

$$\begin{aligned} \phi^{(n)}(\vec{r}^n) &:= -k_B T \ln g^{(n)}(\vec{r}^n) \\ &= U_n + \Delta\Omega - n\mu^{\text{ex}}, \end{aligned} \quad (4)$$

which we call the *generalized potential of mean force*. For the case $n = 2$ this reduces to the usual potential of mean force in the liquid-state literature [34].

This completes our proof that the correlations can be transformed to a potential, and we can proceed with a geometrical construction for $\Delta\Omega$.

B. Representing the insertion cost as a solvation problem

For systems with excluded volume interactions, we can divide the space into a local component $\mathcal{L} \subset \mathbb{R}^d$ of volume $V_{\mathcal{L}}$ inaccessible to solvent degrees of freedom and the remaining space $\mathcal{R} = \mathbb{R}^d \setminus \mathcal{L}$ of volume $V_{\mathcal{R}}$ filled by the rest of the liquid (Fig. 1). The total volume is $V = V_{\mathcal{L}} + V_{\mathcal{R}}$ so the homogeneous grand potential is

$$\Omega_{\text{hom}} = -pV.$$

After inserting the inhomogeneity the total volume accessible to the rest of the liquid will be reduced by $V_{\mathcal{L}}$, so the grand potential becomes

$$\Omega = -pV_{\mathcal{R}} + \Omega_{\text{ex}}[\partial\mathcal{L}],$$

where Ω_{ex} is an excess term brought about by the introduction of a dividing surface $\partial\mathcal{L}$ between the two liquid components. Subtracting these two expressions gives

$$\Delta\Omega := \Omega - \Omega_{\text{hom}} = pV_{\mathcal{L}} + \Omega_{\text{ex}}[\partial\mathcal{L}].$$

This dividing surface has area $A_{\partial\mathcal{L}}$, creating a surface tension γ so we can write the excess term as

$$\Omega_{\text{ex}}[\partial\mathcal{L}] = \gamma[\partial\mathcal{L}]A_{\partial\mathcal{L}},$$

which is a formal definition of surface tension and depends on the choice of dividing surface [see two examples in Fig. 1(b)]. We know from density functional theory [35] that the excess free energy is a functional of the density profile, which will

in turn depend on the shape of the boundary; we write $\gamma = \gamma[\partial\mathcal{L}]$ to indicate this functional dependence on the surface shape. The *solvation form* of the inhomogeneous grand potential term in Eq. (4) is then

$$\Delta\Omega[\mathcal{L}] = pV_{\mathcal{L}} + \gamma[\partial\mathcal{L}]A_{\partial\mathcal{L}}. \quad (5)$$

The problem of determining the n -particle distributions has been reduced to a solvation problem: we must find the surface tension between a solute (the specific local arrangement) and a solvent (the rest of the liquid). We will use the solute–solvent terminology, but one could also think of local–bulk nomenclature.

III. OBTAINING A MORPHOLOGICAL THEORY FOR MANY-BODY CORRELATIONS

We will consider a single-component hard-sphere fluid, for particles of diameter σ and bulk volume fraction η . Using the correspondence between many-body correlation functions and chemical potentials, we require an approximate model for solvation and a choice of surface in Eq. (5) to evaluate $\Delta\Omega$ in Eq. (4). We introduce our central approximation in Sec. III A and our choice of surface in Sec. III B. Then, we show that previous theories fail to produce accurate correlation functions at high densities in Sec. III C and derive a new theory to rectify this in Sec. III D.

A. Our central approximation: the morphometric or scaled-particle ansatz

Our key approximation, the morphometric approach, can be understood as a generalization of scaled-particle theory. In every formulation of scaled-particle theory one considers a hard *spherical* solute of radius R . In most approaches, the cost $\Delta\Omega$ is assumed to have an analytic expansion in powers of the radius; in classical approaches this was simply postulated, however, we will be able provide proper justification below through geometric arguments. Recognising that terms scaling faster than R^3 must be zero for it to remain well-defined in the limit of large solutes leads to the third-order polynomial [16]

$$\Delta\Omega(R) = p\frac{4\pi R^3}{3} + a_2 4\pi R^2 + a_1 4\pi R + a_0 4\pi, \quad (6)$$

where we identified the largest power with the work term pV from comparison with Eq. (5), and $\{a_0, a_1, a_2\}$ are thermodynamic coefficients describing the subleading corrections. We have chosen to introduce factors of 4π in front of the subleading terms to lead into the generalization beyond spherical geometries. For a general solute $K \subset \mathbb{R}^3$ we then write the morphometric insertion cost as

$$\Delta\Omega[K] = pV[K] + a_2 A[K] + a_1 C[K] + a_0 X[K], \quad (7)$$

where C and X are the integrated mean and Gaussian curvatures. For a spherical solute these reduce to the values given in Eq. (6), so this represents a proper generalization of SPT for more general geometries. The *ansatz* Eq. (7) can be justified through integral geometric arguments [6,7].

The key advantage of a geometric expansion of the free energy is that the role of thermodynamics and geometry are kept separate. Thermodynamics only enters through the

coefficients $\{p, a_2, a_1, a_0\}$, so they can be determined in simple geometries to obtain a general theory. As a linear theory, *only* four (independent) equations are required to fix these coefficients; with many thermodynamic relations to choose from this approximate theory is overconstrained in general. We must use physical intuition to choose suitable equations, after which the accuracy of the resulting coefficients can be assessed. After determining these coefficients all the complexity of computing $\Delta\Omega$ is reduced to measuring the geometric quantities $\{V, A, C, X\}$ of the specific solute. However, we must first specify a choice of surface $\partial\mathcal{L}$ in Eq. (5) before we can proceed.

B. Choice of dividing surface

All coefficients we give are for the molecular geometry bounded by the *molecular surface* $[\partial\mathcal{L}_1$ in Fig. 1(b)], the surface where interactions occur between the solute and a test particle representing the remaining liquid. However, it is usually more convenient to do calculations with the excluded geometry: the space inaccessible to the *centre* of a test particle bounded by the *solvent accessible surface* $[\partial\mathcal{L}_2$ in Fig. 1(b)]. Note that there is also an infinite family of well-defined parallel surfaces between these two extremes, but they are not widely used in practice so we will not consider them [10]. The choice of dividing surface will change the surface tension, and thus requires new coefficients $\{a'_0, a'_1, a'_2\}$, i.e.,

$$\Delta\Omega[K] = pV_+[K] + a'_2 A_+[K] + a'_1 C_+[K] + a'_0 X_+[K], \quad (8)$$

where the excluded geometry terms transform via the canonical relations [10,30,36,37]

$$X_+[K] = X[K], \quad (9a)$$

$$C_+[K] = C[K] + \frac{\sigma}{2} X[K], \quad (9b)$$

$$A_+[K] = A[K] + \sigma C[K] + \frac{\sigma^2}{4} X[K], \quad (9c)$$

$$V_+[K] = V[K] + \frac{\sigma}{2} A[K] + \frac{\sigma^2}{4} C[K] + \frac{\sigma^3}{24} X[K]. \quad (9d)$$

It is straightforward to transform between these two conventions via [10,30]

$$a'_0 = a_0 - \frac{\sigma}{2} a_1 + \frac{\sigma^2}{4} a_2 - \frac{\sigma^3}{24} p, \quad (10a)$$

$$a'_1 = a_1 - \sigma a_2 + \frac{\sigma^2}{4} p, \quad (10b)$$

$$a'_2 = a_2 - \frac{\sigma}{2} p. \quad (10c)$$

The resulting $\Delta\Omega$ will be identical whichever surface is chosen, except when there is a topological change in the molecular surface marking the breakdown of the theory; this is discussed in detail in Ref. [10].

C. Failure of previous morphometric theories in treating correlations

Having specified the surface, we can examine the self-consistency of correlation functions determined through previously known morphological theories. We briefly state the

main theories below, then proceed to show how they produce inaccurate correlation functions at high densities. This underscores the need for a more accurate theory, and the specific inconsistency we highlight in this section will be used to construct one in the next section.

With either the scaled particle or morphometric *ansatzes*, Eq. (6) or Eq. (7), a specific theory comprises the set of coefficients $\{p, a_2, a_1, a_0\}$. In Appendix A we summarize the classical scaled-particle arguments of Refs. [16,24] using modern notation, which produce coefficients

$$\beta a_0^{\text{SPT/PY}} = -\frac{\ln(1-\eta)}{4\pi}, \quad (11a)$$

$$\beta a_1^{\text{SPT/PY}} = \frac{3\eta}{2\pi\sigma(1-\eta)}, \quad (11b)$$

$$\beta a_2^{\text{SPT/PY}} = \frac{6\eta + 3\eta^2}{2\pi\sigma^2(1-\eta)^2}, \quad (11c)$$

$$\frac{\beta p^{\text{SPT/PY}}}{\rho} = \frac{1 + \eta + \eta^2}{(1-\eta)^3}. \quad (11d)$$

In this classical approach, the Percus-Yevick (PY) equation of state emerges as an *output* of the theory. More recently, morphometric theories have been obtained as the bulk limit of FMT, with the hitherto most successful theory determined in Ref. [30] as

$$\beta a_0^{\text{SPT/CS}} = -\frac{\ln(1-\eta)}{4\pi}, \quad (12a)$$

$$\beta a_1^{\text{SPT/CS}} = \frac{1}{2\pi\sigma} \left[\frac{5\eta + \eta^2}{1-\eta} + 2\ln(1-\eta) \right], \quad (12b)$$

$$\beta a_2^{\text{SPT/CS}} = \frac{1}{\pi\sigma^2} \left[\frac{\eta(2 + 3\eta - 2\eta^2)}{(1-\eta)^2} - \ln(1-\eta) \right], \quad (12c)$$

$$\frac{\beta p^{\text{SPT/CS}}}{\rho} = \frac{1 + \eta + \eta^2 - \eta^3}{(1-\eta)^3}, \quad (12d)$$

obtained from a functional constructed to impose the Carnahan-Starling (CS) equation of state Eq. (12d). The latter equation of state is known to be highly accurate across the whole stable liquid regime, and even at the high density limits accessible to simulation in the supercooled regime [38]. The same equations are also obtained in the bulk limit of the functional of Ref. [39], which similarly imposes the CS pressure but is slightly more self-consistent. Curiously, we can make a minor modification to SPT arguments to impose the CS equation of state as an *input* to obtain the above coefficients without invoking FMT (details in Appendix B). We thus label this theory as SPT/CS.

To demonstrate the inaccuracy of the correlation functions produced by these known theories using Eq. (3), we consider what happens to the pair correlation at high densities. The potential of mean force Eq. (4) for nonoverlapping spheres with the morphometric *ansatz* Eq. (7) is written

$$\begin{aligned} \phi^{(2)}(r) &:= -k_B T \ln g^{(2)}(r) \\ &= pV(r) + a_2 A(r) + a_1 C(r) + a_0 X(r) - 2\mu^{\text{ex}}[p]. \end{aligned} \quad (13)$$

As a self-consistency test, we will compare this explicit result at contact against the *exact* value of $g^{(2)}(\sigma)$ predicted by the

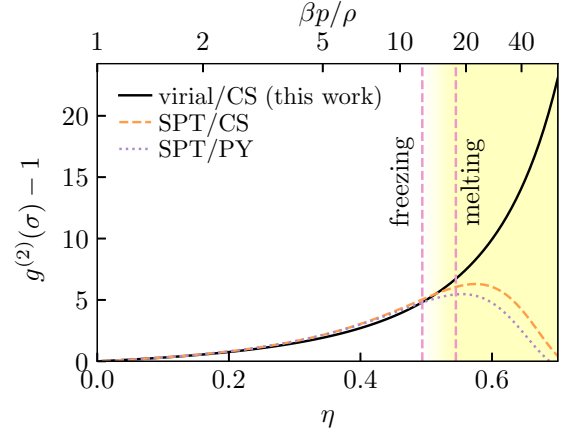


FIG. 2. Contact values of the radial distribution function against volume fraction η and reduced pressure for the hard-sphere liquid with Eqs. (3) and (7) for the explicit form of $g^{(2)}$, assuming the Carnahan-Starling (CS) and scaled-particle theory and Percus-Yevick (SPT/PY) equations of state. Contact values are determined with three sets of morphometric coefficients: virial/CS, derived in this work to be quasixact [i.e., satisfying the virial theorem (14)] by construction; SPT/CS, a generalization of scaled-particle theory which imposes the CS equation of state; and SPT/PY, the classical scaled-particle solution. The latter two scaled-particle theories feature a spurious decay in the supercooled regime (shaded area). The hard-sphere freezing and melting volume fractions are indicated by pink dashed lines to show the onset of the supercooled regime.

virial theorem as [34]

$$g^{(2)}(\sigma) = \frac{3}{2\pi\sigma^3\rho} \left(\frac{\beta p}{\rho} - 1 \right). \quad (14)$$

To evaluate Eq. (13) we need to calculate the size measures for the two particle solute resembling a “dumbbell.” It is easier to calculate these for the excluded volume geometry, after which we can obtain the molecular volumes using the canonical relations Eq. (9). The excluded volume consists of the union of two balls of radius σ separated by a distance r . The geometric properties at contact are then [10]

$$\begin{aligned} X_+(\sigma) &= 4\pi, \\ C_+(\sigma) &= \left(6 - \frac{\pi}{2\sqrt{3}} \right) \pi\sigma, \\ A_+(\sigma) &= 6\pi\sigma^2, \\ V_+(\sigma) &= \frac{9\pi\sigma^3}{4}. \end{aligned}$$

Transforming to the parallel molecular surface using the inverse transformation of Eq. (9) gives the solute parameters as

$$C(\sigma) = \left(4 - \frac{\pi}{2\sqrt{3}} \right) \pi\sigma, \quad (15a)$$

$$A(\sigma) = \left(1 + \frac{\pi}{2\sqrt{3}} \right) \pi\sigma^2, \quad (15b)$$

$$V(\sigma) = \left(\frac{7}{12} - \frac{\pi}{8\sqrt{3}} \right) \pi\sigma^3. \quad (15c)$$

Figure 2 shows the contact value $g^{(2)}(\sigma)$ from inserting these geometric parameters into Eq. (13), and the quasixact result of Eq. (14) assuming the CS equation of state Eq. (12d).

We find that both known morphometric theories Eqs. (11) and (12) are reasonably accurate until around the freezing density, above which contact correlations spuriously decay. Thus, a new theory is needed to treat correlations at high densities; in the next section we will construct one which satisfies Eq. (14) by construction.

D. Obtaining the new theory by self-consistency of the contact value of $g^{(2)}(r)$ with the virial theorem

Our goal is to develop a morphometric theory which produces accurate correlation functions $g^{(n)}$. As described at the

$$p\left(\frac{7}{12} - \frac{\pi}{8\sqrt{3}}\right)\pi\sigma^3 + a_2\left(1 + \frac{\pi}{2\sqrt{3}}\right)\pi\sigma^2 + a_1\left(4 - \frac{\pi}{2\sqrt{3}}\right)\pi\sigma + a_0 4\pi = 2\mu^{\text{ex}}[p] - \beta^{-1} \ln \frac{3}{2\pi\rho\sigma^3} \left(\frac{\beta p}{\rho} - 1\right). \quad (16)$$

We will use this last expression instead of the contact theorem Eq. (A4) in order to obtain new coefficients. Together Eqs. (A2a), (A3), and (16) solve to give coefficients

$$\beta a_0^{\text{virial}} = -\frac{\ln(1-\eta)}{4\pi}, \quad (17a)$$

$$\beta a_1^{\text{virial}} = \frac{1}{(\sqrt{3}\pi - 4)\pi\sigma} \left[\left(5 - \frac{5\pi}{2\sqrt{3}}\right)\eta \frac{\beta p}{\rho} - \left(2 - \frac{\pi}{\sqrt{3}}\right)\beta\mu^{\text{ex}}[p] + \frac{\pi}{\sqrt{3}} \ln(1-\eta) + 2 \ln\left(\frac{\beta p}{\rho} - 1\right) \right], \quad (17b)$$

$$\beta a_2^{\text{virial}} = -\frac{1}{(\sqrt{3}\pi - 4)\pi\sigma^2} \left[\left(6 - \frac{2\pi}{\sqrt{3}}\right)\eta \frac{\beta p}{\rho} - \frac{\pi}{\sqrt{3}}\beta\mu^{\text{ex}}[p] + \left(4 - \frac{\pi}{\sqrt{3}}\right) \ln(1-\eta) + 4 \ln\left(\frac{\beta p}{\rho} - 1\right) \right]. \quad (17c)$$

We refer to coefficients obtained this way for the CS pressure (12d) as virial/CS, but we will not give them explicitly. Unlike the WBII coefficients above these are new. The pair correlation produced by these coefficients (black line in Fig. 2) is self-consistent with CS at contact by construction.

IV. NUMERICAL RESULTS

We apply the thermodynamic coefficients determined in previous sections for a system of hard spheres to obtain two- and three-body distribution functions using the generalized potential of mean force Eq. (4) with the morphometric approach Eq. (7), and compare these against molecular dynamics simulations. For the analytics we determine the input geometric quantities $\{V, A, C, X\}$ using the algorithms of Refs. [41,42]. For the simulations we performed event-driven molecular dynamics of $N = 1372$ monodisperse hard spheres using the DynamO software package [43]. We measure the pair and triplet distribution functions $g^{(2)}$ and $g^{(3)}$ for simulations at $\eta = 0.45$. For simulations above freezing $\eta \simeq 0.494$ we used a five-component equimolar distribution with $\sim 8\%$ polydispersity.

For $g^{(2)}$ shown in Fig. 3 we find the virial/CS theory outperforms the SPT/CS theory even away from contact. The agreement with the molecular dynamics simulations is excellent, until $r \gtrsim \sqrt{3}\sigma$, where the solute boundary self-intersects marking the end of the theory's regime of validity. Geometrically, the regime $r < \sqrt{3}\sigma$ is the regime where the canonical relations Eq. (9) apply so the thermodynamics is independent of the choice of surface definition. Physically, for $r > \sqrt{3}\sigma$ interactions between solvent particles can occur

end of the last section, the correlation functions produced by an SPT approach are inaccurate at high densities. We will correct the spurious decay of the contact value of the pair distribution function $g^{(2)}(r)$ at high densities by building this into the theory explicitly, with the aim of producing more accurate correlation functions. A working understanding of scaled-particle arguments is necessary to follow the details of this derivation, which we lay out in Appendices A and B.

Inserting the volumes at contact Eq. (15) into Eq. (13) and applying the virial theorem Eq. (14) for the contact value of $g^{(2)}$ gives the final expression

through the solute, and these correlations are not captured by the theory. More discussion of this breakdown can be found in Ref. [10]. Only the contact value was fixed, so accuracy for $r > \sigma$ was not guaranteed; the accuracy is a welcome bonus.

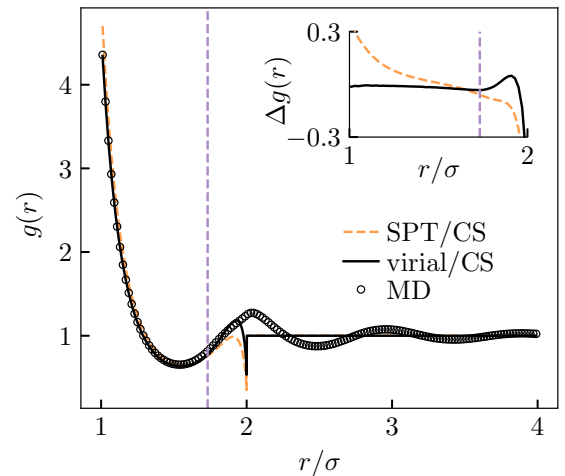


FIG. 3. Comparing radial distribution functions of the morphometric theories which impose the Carnahan-Starling equation of state Eq. (12d), against results of molecular dynamics (MD) simulations at volume fraction $\eta = 0.45$. The inset shows the difference between the two theoretical distribution functions and the molecular dynamics. The purple dashed line indicates where the molecular surface self-intersects at $r = \sqrt{3}\sigma$, marking the end of the theory's regime of validity.

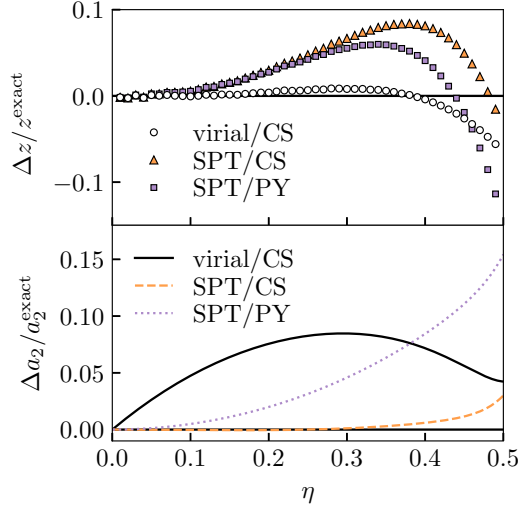


FIG. 4. Errors in different morphometric theories for hard spheres. Top panel: error in the coordination defined in Eq. (18), giving the average number of neighbours in the shell $r < 1.4\sigma$ around a particle. Bottom panel: planar surface tensions against volume fraction, using the highly accurate result Eq. (19) from Ref. [40] valid until $\eta \sim 0.5$.

We can quantify this accuracy through the integrated value

$$z(\delta) = 4\pi \int_{\sigma}^{\sigma+\delta} \rho^{(2)}(r) r^2 dr \quad (18)$$

shown in the top panel of Fig. 4 where we take $\delta = 0.4\sigma$. We find this integrated quantity is within 10% accuracy across the liquid regime for all three theories, with the new theory performing substantially better overall. Despite the improved accuracy, the errors begin to increase in magnitude at the end of the liquid regime so we expect them to become significant with very deep supercooling.

Next we compare the theories' predicted surface tension against simulation data. The surface tension at a planar wall is simply a_2 because it conjugates with the area. In Ref. [40] a highly accurate a_2 was measured for hard spheres through extensive simulation, which was parameterised by the following expression:

$$\beta a_2 = \frac{1}{\pi \sigma^2} \left[\frac{\eta(2 + 3\eta - \frac{9}{5}\eta^2 - \frac{4}{3}\eta^3 - (5 \times 10^4)\eta^{20})}{(1 - \eta)^2} - \ln(1 - \eta) \right]. \quad (19)$$

Comparing this highly accurate expression against the values predicted from the morphometric coefficients, we find the virial/CS surface tension is less accurate than the SPT/CS prediction (Fig. 4 bottom panel) despite its superior correlation functions at high densities. Moreover, we find that at low densities the new theory is less accurate than classical SPT/PY theory. This discrepancy occurs because both SPT/PY and SPT/CS feature the correct low density asymptotics of $a_2 \sim \mathcal{O}(\eta)$, which is imposed through the radial derivative of $\Delta\Omega(r)$ in the point solute limit Eq. (A2b). This suggests that the new virial/CS theory sacrifices asymptotic accuracy at low densities, for more self-consistency

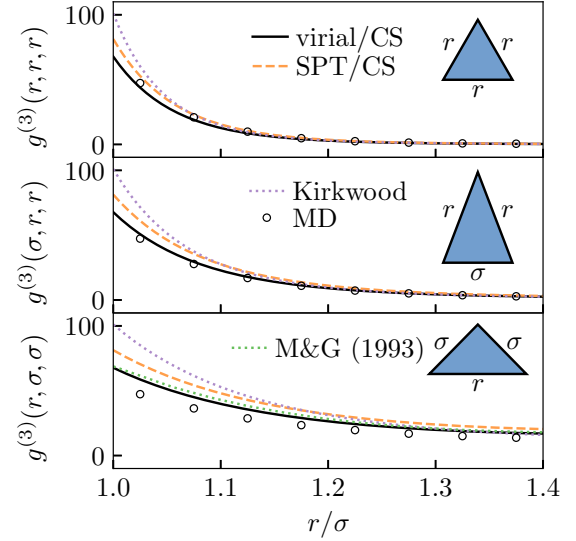


FIG. 5. Comparison of predicted correlations for the morphometric approaches in triangular geometries, i.e., the first correlations beyond the pair level, against molecular dynamics simulations at volume fraction $\eta = 0.45$. In the bottom panel we also include the tabulated values of Ref. [44] for comparison.

of the surface tension at moderate to high densities. One of the great strengths of the SPT/CS theory is its accuracy in the planar limit [30], and so SPT/CS coefficients may give more accurate grand potentials (and thus correlations) for large solutes where the surface becomes approximately planar.

Our goal was to develop a theory capable of treating correlations at the many-body level, so we now examine three-body correlation functions. Triplet geometries are characterised by a triangle of side lengths r, s, t so $g^{(3)} = g^{(3)}(r, s, t)$. We also compare the morphometric theories against the Kirkwood approximation [1], i.e.,

$$g^{(3)}(r, s, t) \approx g^{(2)}(r)g^{(2)}(s)g^{(2)}(t), \quad (20)$$

where we take the values of $g^{(2)}$ from the virial/CS theory because of its already demonstrated accuracy at the two body level. Comparison of the morphometric correlation functions, and the Kirkwood closure, against molecular dynamics are shown in Fig. 5. The virial/CS closure most closely matches the simulations at high densities, suggesting the theory is suitable for modeling complex many-particle local structures [6]. For comparison we also include the tabulated values of Ref. [44], where $g^{(3)}$ is used to treat polyatomic molecules [46]; our theory is marginally more accurate, and more importantly it provides a recipe for treating the higher-order correlation functions.

To quantify accuracy at the three-body level we consider the concentration of triangles with side lengths $r, s, t \in [\sigma, \sigma + \delta]$ in the bulk liquid, from Eq. (1) we find this as [47]

$$C_{\Delta}(\delta) = 8\pi^2 \int_{\sigma}^{\sigma+\delta} \int_{\sigma}^{\sigma+\delta} \int_{\sigma}^{\sigma+\delta} \rho^{(3)}(r, s, t) rst dr ds dt. \quad (21)$$

Comparison with molecular dynamics simulations in Fig. 6 shows similar levels of accuracy for small δ , though the performance decreases as it is increased above the first minimum

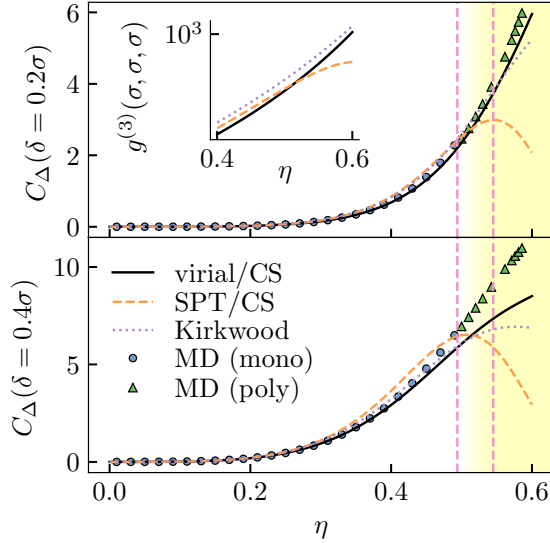


FIG. 6. Concentration of triangles in the hard-sphere liquid with side lengths $r, s, t \in [\sigma, \sigma + \delta]$ versus volume fraction. Direct measurements by molecular dynamics using a single-component system and an 8% polydisperse system, while the lines show predictions from the morphometric theories described in text. The hard-sphere freezing and melting volume fractions are indicated by pink dashed lines to show the onset of the supercooled regime. Inset: contact value of $g^{(3)}$ showing how the errors in the SPT/CS theory arise from underestimation close to contact.

of the $g^{(2)}(r)$; this is not surprising as our virial closure only enforces accuracy approaching contact. Notably, the Kirkwood approximation Eq. (20) performs surprisingly well at the three-body level in both of these tests.

V. DISCUSSION AND SUMMARY

We have presented the morphometric approach as a generalization of SPT, thus placing the scaled-particle *ansatz* on more precise and physically motivated assumptions, i.e., those underlying the theorems of integral geometry. Using the scaled-particle approach we have systematically derived a new theory capable of accurately calculating many-body correlations in the hard-sphere liquid; we recently used this to accurately treat local structures in Ref. [6]. Our scaled-particle formalism is flexible enough to derive all known morphometric theories without involving fundamental measure theory.

In principle this approach could be extended to simple liquids where the interaction potential can be approximated as a perturbation around a hard core. However, as we exploited features of the hard-sphere interaction potential to achieve closed form expressions, more realistic interaction potentials would likely require numerical expressions. Additionally, attractions can introduce nonanalytic behavior surface phase transitions not present in our theory [48,49].

By making the underlying assumptions explicit we can better understand the limits of the theory: any deviation from the morphometric/SPT *ansatz* must be due to a violation of translation or rotation invariance, additivity or continuity [7]. The fact that these theories are very accurate for hard spheres suggests that the assumptions are only weakly violated for

this system. While translational or rotational invariance and continuity are physically plausible conditions on $\Delta\Omega$, additivity is a very strong assumption. In particular, we expect significant deviations from additivity where the liquid develops a static length scale exceeding the size of the solute [7]. As such, we expect the validity of the morphometric approach to require the solute to be larger than the point-to-set length [50], which acts as an upper bound for all structural length scales [51]. The morphometric *ansatz* must break down approaching a critical point, so it cannot be used to obtain asymptotics in the event of a thermodynamic glass transition.

Finally, we remark that while it is tempting to call the treatment of bulk degrees of freedom with the morphometric approach mean-field, this would not be completely accurate. Mean-field theories typically become formally exact in the limit of infinite spatial dimensions, where the thermodynamic role of fluctuations disappears. By contrast, the morphometric approach (and related theories like SPT and FMT) become formally exact in the one-dimensional limit of hard rods. Though this theory does not explicitly describe fluctuations, they are built into the choice of thermodynamic coefficients. In this sense it is more accurate to describe the morphometric approach (and related theories) as an *excluded volume* theory, or as a *free volume* theory because the thermodynamics only shows divergent behavior as $\eta \rightarrow 1$.

ACKNOWLEDGMENTS

We are grateful to Bob Evans who encouraged writing up the results of Sec. III, which eventually became this manuscript. J.F.R., F.T., and C.P.R. acknowledge the European Research Council under the FP7/ERC Grant Agreement No. 617266 “NANOPRS.” C.P.R. acknowledges the Royal Society for financial support.

APPENDIX A: CLASSICAL SCALED-PARTICLE RELATIONS

Following the protocol of scaled-particle theories, we consider the insertion of a hard spherical solute of radius R into the liquid. Assuming the morphometric form for the insertion cost returns us to the *ansatz* Eq. (6). Below we give the exact thermodynamic relations for hard spheres which produce the classical SPT coefficients.

It is possible to consider the insertion of a solute with a *negative* radius: The hard core interaction between the two particles only occurs when the solute is “inside” a solvent particle. In this limit the insertion cost can be determined exactly as [16]

$$\beta \Delta\Omega = -\ln \left[1 - \frac{4\pi \left(R + \frac{\sigma}{2}\right)^3}{3} \rho \right] \quad (\text{A1})$$

for $-\frac{\sigma}{2} \leq R \leq 0$. It may appear concerning that this result does not possess the morphometric form Eq. (7); however, this does not discount the validity of the morphometric approach as the nonphysical geometry violates the continuity assumption [7] because it cannot be approximated by polyhedra. This places the result for $R < 0$ outside the theory’s stated regime of validity, however $\Delta\Omega$ is continuous up to its second

derivative across $R = 0$ with a discontinuity in its third derivative [16]. In the limit $R \rightarrow 0$ the expression above corresponds to the cost of inserting a hard point, giving

$$\beta \Delta \Omega(R = 0) = -\ln(1 - \eta), \quad (\text{A2a})$$

$$\beta \left(\frac{\partial \Delta \Omega}{\partial R} \right)_{\mu, \nu, T} \Big|_{R=0} = \frac{6\eta}{\sigma(1 - \eta)}, \quad (\text{A2b})$$

$$\beta \left(\frac{\partial^2 \Delta \Omega}{\partial R^2} \right)_{\mu, \nu, T} \Big|_{R=0} = \frac{12\eta^2 + 24\eta}{\sigma^2(1 - \eta)^2}. \quad (\text{A2c})$$

Note that Eq. (A2a) can also be justified by considering that the probability of a randomly selected position in space being empty is simply the free volume $1 - \eta$.

Together applying Eq. (A2) to Eq. (6) fixes the coefficients $\{a_0, a_1, a_2\}$, so the theory requires an additional thermodynamic relation to determine the pressure. When $R = \frac{\sigma}{2}$ the solute is equivalent to the solvent particles themselves and we recover $\Delta \Omega = \mu^{\text{ex}}$, so from Eq. (6) we have

$$\Delta \Omega \left(R = \frac{\sigma}{2} \right) = \frac{\pi \sigma^3}{6} p + \pi \sigma^2 a_2 + 2\pi \sigma a_1 + 4\pi a_0 = \mu^{\text{ex}}. \quad (\text{A3})$$

Combining this expression with the thermodynamic relation Eq. (B1) gives a differential equation for βp whose solution gives the classical SPT coefficients for hard spheres [Eq. (11)]. The equation of state Eq. (11d) is equivalent to the one obtained through the solution of the Percus-Yevick (PY) integral equation [17]; these two routes have been unified within FMT [18].

A final thermodynamic relation can be determined as [6,52]

$$\beta \left(\frac{\partial \Delta \Omega}{\partial R} \right)_{\mu, \nu, T} \Big|_{R=\frac{\sigma}{2}} = 4\pi \sigma^2 \rho g^{(2)}(\sigma).$$

So inserting the SPT *ansatz* Eq. (6) gives

$$\pi \sigma^2 p + 4\pi \sigma a_2 + 4\pi a_1 = \frac{6}{\beta \sigma} \left(\frac{\beta p}{\rho} - 1 \right), \quad (\text{A4})$$

after inserting the virial theorem Eq. (14). This relation is satisfied by the coefficients Eq. (11), which is surprising given that it was obtained from a completely different thermodynamic route and the *ansatz* Eq. (6) is inexact. Nonetheless, this self-consistency is a testament to the effectiveness of SPT and related approaches.

APPENDIX B: FIRST GENERALIZATION: SPT WITH AN EMPIRICAL EQUATION OF STATE

In the classical SPT approach described in the previous section, the SPT/PY equation of state emerges as an *output* of the theory. Taking inspiration from the White Bear free-energy functional [53], we reformulate the SPT argument so that the equation of state is an *input* to the theory. In so doing we aim to construct a theory from a more accurate equation of state, with the trade-off being that we must sacrifice some self-consistency. The main equation of state we impose is the CS relation Eq. (12d) [54]. This ultimately results in a theory

previously known as a limit of a free-energy functional [30], but through simpler arguments. We extend these arguments in the main text to arrive at a new theory capable of accurately treating correlation functions.

Since the pressure is now a known input, the excess chemical potential can be determined via

$$\beta \mu^{\text{ex}}[p] = \left(\frac{\beta p}{\rho} - 1 \right) + \int_0^\eta \left(\frac{\beta p}{\rho} - 1 \right) \frac{d\eta'}{\eta'}. \quad (\text{B1})$$

With the pressure fixed we have three free parameters in the theory $\{a_0, a_1, a_2\}$; we must thus choose three out of the five available thermodynamic relations in Eqs. (A2), (A3), and (A4) to satisfy. Therefore, we must lose consistency with two of these relations to obtain a more accurate theory for practical applications.

To set the correct energy scale we choose to fix $\Delta \Omega(R = 0)$ and $\Delta \Omega(R = \sigma/2)$ through Eqs. (A2a) and (A3) using the chemical potential determined by Eq. (B1). This in turn imposes the consistency of the osmotic pressure Eq. (B1). For the final equation we choose to set the contact value of $g^{(2)}$ through Eq. (A4) which better represents solutes of interest than the two relations for point geometries at $R = 0$. Solving these three equations gives the generalized SPT coefficients

$$\beta a_0^{\text{SPT}} = -\frac{\ln(1 - \eta)}{4\pi}, \quad (\text{B2a})$$

$$\beta a_1^{\text{SPT}} = \frac{1}{2\pi \sigma} \left[(\eta - 3) \frac{\beta p}{\rho} + 2\beta \mu^{\text{ex}}[p] + 2\ln(1 - \eta) + 3 \right], \quad (\text{B2b})$$

$$\beta a_2^{\text{SPT}} = -\frac{1}{\pi \sigma^2} \left[(2\eta - 3) \frac{\beta p}{\rho} + \beta \mu^{\text{ex}}[p] + \ln(1 - \eta) + 3 \right]. \quad (\text{B2c})$$

It can be verified that inserting the Percus-Yevick equation of state Eq. (11d) into these expressions yields the previously obtained coefficients Eq. (11), as expected. Inserting the CS equation of state we obtain Eq. (12) which are *identical* to the coefficients derived from the White Bear II (WBII) free-energy functional of Ref. [30], although this is only clear after transforming to the excluded geometry through the canonical relations Eq. (10). Remarkably, we have obtained these coefficients through a route completely different from their original derivation.

In Ref. [30] the coefficients were determined within FMT by taking the limit of a binary mixture where one component is infinitely dilute. Here we completely avoided FMT, in favour of geometrical arguments similar to the classical SPT approach outlined in the previous section. This suggests that this generalized scaled-particle argument is built into the structure of the WBII functional of Ref. [30]; this is not an obvious fact as the derivation of this functional did not explicitly involve these arguments. Rather, the WBII functional was constructed based on a novel extension of the CS equation to mixtures by requiring self-consistency of the osmotic pressure [55]. We imposed this relation by setting the chemical potential in Eq. (A3) using Eq. (B1). It is unclear to us how our final choice of using Eq. (A3) instead of one of the two relations at the origin, i.e., Eq. (A2b) or Eq. (A2c), is built into the WBII functional.

- [1] J. G. Kirkwood, *J. Chem. Phys.* **3**, 300 (1935).
- [2] R. P. Sear, *J. Phys. Condens. Matter* **19**, 033101 (2007).
- [3] V. Lubchenko and P. G. Wolynes, *Annu. Rev. Phys. Chem.* **58**, 235 (2007).
- [4] C. Brito and M. Wyart, *J. Chem. Phys.* **131**, 024504 (2009).
- [5] D. Chandler and J. P. Garrahan, *Annu. Rev. Phys. Chem.* **61**, 191 (2010).
- [6] J. F. Robinson, F. Turci, R. Roth, and C. P. Royall, *Phys. Rev. Lett.* **122**, 068004 (2019).
- [7] P.-M. König, R. Roth, and K. R. Mecke, *Phys. Rev. Lett.* **93**, 160601 (2004).
- [8] R. Roth, Y. Harano, and M. Kinoshita, *Phys. Rev. Lett.* **97**, 078101 (2006).
- [9] H. Hansen-Goos, R. Roth, K. R. Mecke, and S. Dietrich, *Phys. Rev. Lett.* **99**, 128101 (2007).
- [10] M. Oettel, H. Hansen-Goos, P. Bryk, and R. Roth, *Europhys. Lett.* **85**, 36003 (2009).
- [11] D. J. Ashton, N. B. Wilding, R. Roth, and R. Evans, *Phys. Rev. E* **84**, 061136 (2011).
- [12] B. B. Laird, A. Hunter, and R. L. Davidchack, *Phys. Rev. E* **86**, 060602(R) (2012).
- [13] E. M. Blokhuis, *Phys. Rev. E* **87**, 022401 (2013).
- [14] I. Urrutia, *Phys. Rev. E* **89**, 032122 (2014).
- [15] H. Hansen-Goos, *J. Chem. Phys.* **141**, 171101 (2014).
- [16] H. Reiss, H. L. Frisch, and J. L. Lebowitz, *J. Chem. Phys.* **31**, 369 (1959).
- [17] M. S. Wertheim, *Phys. Rev. Lett.* **10**, 321 (1963).
- [18] Y. Rosenfeld, *Phys. Rev. Lett.* **63**, 980 (1989).
- [19] H. Reiss, H. L. Frisch, E. Helfand, and J. L. Lebowitz, *J. Chem. Phys.* **32**, 119 (1960).
- [20] E. Helfand, H. Reiss, H. L. Frisch, and J. L. Lebowitz, *J. Chem. Phys.* **33**, 1379 (1960).
- [21] H. Reiss and S. W. Mayer, *J. Chem. Phys.* **34**, 2001 (1961).
- [22] R. Gibbons, *Mol. Phys.* **17**, 81 (1969).
- [23] R. Gibbons, *Mol. Phys.* **18**, 809 (1970).
- [24] J. L. Lebowitz, E. Helfand, and E. Praestgaard, *J. Chem. Phys.* **43**, 774 (1965).
- [25] F. H. Stillinger, P. G. Debenedetti, and S. Chatterjee, *J. Chem. Phys.* **125**, 204504 (2006).
- [26] S. Chatterjee, P. G. Debenedetti, and F. H. Stillinger, *J. Chem. Phys.* **125**, 204505 (2006).
- [27] E. Helfand, H. L. Frisch, and J. L. Lebowitz, *J. Chem. Phys.* **34**, 1037 (1961).
- [28] S. C. Martin, B. B. Laird, R. Roth, and H. Hansen-Goos, *J. Chem. Phys.* **149**, 084701 (2018).
- [29] H. Hansen-Goos, *J. Chem. Phys.* **150**, 011101 (2019).
- [30] H. Hansen-Goos and R. Roth, *J. Phys. Condens. Matter* **18**, 8413 (2006).
- [31] B. Widom, *J. Chem. Phys.* **39**, 2808 (1963).
- [32] B. Widom, *J. Phys. Chem.* **86**, 869 (1982).
- [33] J. S. Rowlinson and B. Widom, *Molecular Theory of Capillarity* (Dover Publications, Mineola, NY, 2002).
- [34] J.-P. Hansen and I. R. McDonald, *Theory of Simple Liquids*, 4th ed. (Elsevier, Amsterdam, 2013).
- [35] R. Evans, *Adv. Phys.* **28**, 143 (1979).
- [36] L. A. Santaló, *Integral Geometry and Geometric Probability*, 2nd ed., Cambridge Mathematical Library (Cambridge University Press, Cambridge/New York, 2004).
- [37] D. A. Klain and G.-C. Rota, *Introduction to Geometric Probability* (Cambridge University Press, Cambridge/New York, 1997).
- [38] L. Berthier, D. Coslovich, A. Ninarello, and M. Ozawa, *Phys. Rev. Lett.* **116**, 238002 (2016).
- [39] A. Santos, *Phys. Rev. E* **86**, 040102(R) (2012).
- [40] R. L. Davidchack, B. B. Laird, and R. Roth, *Mol. Phys.* **113**, 1091 (2015).
- [41] K. R. Mecke, T. Buchert, and H. Wagner, *Astron. Astrophys.* **288**, 697 (1994).
- [42] K. V. Klenin, F. Tristram, T. Strunk, and W. Wenzel, *J. Comput. Chem.* **32**, 2647 (2011).
- [43] M. N. Bannerman, L. Lue, and L. V. Woodcock, *J. Chem. Phys.* **132**, 084507 (2010).
- [44] E. A. Müller and K. E. Gubbins, *Mol. Phys.* **80**, 957 (1993).
- [45] P. Attard and G. Stell, *Chem. Phys. Lett.* **189**, 128 (1992).
- [46] We believe there is a misprint in Eq. (A1) of Ref. [44], which should read $(1 - \eta)^3$ in the denominator. We refitted their source data [45] with this corrected form to be sure.
- [47] J. A. Krumhansl and S. S. Wang, *J. Chem. Phys.* **56**, 2034 (1972).
- [48] R. Evans, R. Roth, and P. Bryk, *Europhys. Lett.* **62**, 815 (2003).
- [49] R. Evans, J. R. Henderson, and R. Roth, *J. Chem. Phys.* **121**, 12074 (2004).
- [50] A. Montanari and G. Semerjian, *J. Stat. Phys.* **125**, 23 (2006).
- [51] S. Yaida, L. Berthier, P. Charbonneau, and G. Tarjus, *Phys. Rev. E* **94**, 032605 (2016).
- [52] P. Bryk, R. Roth, K. R. Mecke, and S. Dietrich, *Phys. Rev. E* **68**, 031602 (2003).
- [53] R. Roth, R. Evans, A. Lang, and G. Kahl, *J. Phys. Condens. Matter* **14**, 12063 (2002).
- [54] N. F. Carnahan and K. E. Starling, *J. Chem. Phys.* **51**, 635 (1969).
- [55] H. Hansen-Goos and R. Roth, *J. Chem. Phys.* **124**, 154506 (2006).